Multibody Syst Dyn
DOI 10.1007/s11044-007-9070-6

Effect of the centrifugal forces on the finite element eigenvalue solution of a rotating blade: a comparative study

Luis G. Maqueda · Olivier A. Bauchau · Ahmed A. Shabana

Received: 28 November 2006 / Accepted: 21 May 2007

Abstract In this study, the effect of the centrifugal forces on the eigenvalue solution obtained using two different nonlinear finite element formulations is examined. Both formulations can correctly describe arbitrary rigid body displacements and can be used in the large deformation analysis. The first formulation is based on the *geometrically exact beam theory*, which assumes that the cross section does not deform in its own plane and remains plane after deformation. The second formulation, the *absolute nodal coordinate formulation* (ANCF), relaxes this assumption and introduces modes that couple the deformation of the cross section and the axial and bending deformations. In the absolute nodal coordinate formulation, four different models are developed; a beam model based on a general continuum mechanics approach, a beam model based on an elastic line approach, a beam model based on an elastic line approach combined with the Hellinger–Reissner principle, and a plate model based on a general continuum mechanics approach. The use of the general continuum mechanics approach leads to a model that includes the *ANCF coupled deformation modes*. Because of these modes, the continuum mechanics model differs from the models based on the elastic line approach. In both the geometrically exact beam and the absolute nodal coordinate formulations, the centrifugal forces are formulated in terms of the element nodal coordinates. The effect of the centrifugal forces on the *flap* and *lag modes* of the rotating beam is examined, and the results obtained using the two formulations are compared for different values of the beam angular velocity. The numerical comparative study presented in this investigation shows that when the effect of the ANCF coupled deformation modes is neglected, the eigenvalue solutions obtained using the geometrically exact beam and the absolute nodal coordinate formulations are in a good agreement. The results also show that as the effect of the centrifugal forces, which tend to increase the beam stiffness, increases; the effect of the ANCF coupled deformation modes on the computed eigenvalues becomes

L.G. Maqueda · A.A. Shabana (✉)
Department of Mechanical Engineering, University of Illinois at Chicago, 842 West Taylor Street, Chicago, IL 60607, USA
e-mail: ahmed.a.shabana@uic.edu

O.A. Bauchau
Daniel Guggenheim School of Aerospace Engineering, Georgia Institute of Technology, 270 Ferst Street, Atlanta, GE 30332-0150, USA

« MUBO 11044 layout: Small Condensed v.1.2 reference style: mathphys file: mubo9070.tex (Aiste) aid: 9070 doctopic: OriginalPaper class: spr-small-v1.1 v.2007/06/28 Prn:28/06/2007; 15:52 p. 2»

less significant. In the geometrically exact beam models, the two components of the normal strains associated with the deformation of the cross section are assumed to be zero, and as a consequence, the Poisson ratio effect is not considered. It is shown in this paper that when the effect of the Poisson ration is neglected, the eigenvalue solution obtained using the absolute nodal coordinate formulation and the general continuum mechanics approach is in a good agreement with the solution obtained using the geometrically exact beam model.

Keywords ???

1 Introduction

The dynamics of rotating beams has been the subject of a large number of investigations because of its relevance to important engineering applications such as helicopters' blades. One of the earliest studies is the work of Schilhans [14], who presented the partial differential equation of the flexural vibration of a rotating beam in the steady state. The early investigations were concerned with one-dimensional beam in steady state motion where neither the Coriolis effect nor the coupling between extension and bending were considered. The significant effect of the coupling between the beam extension and bending was recognized, and it was demonstrated that the neglect of the effect of the geometric centrifugal stiffening that results from this coupling leads to incorrect solutions. Johnson [10] documented the need for considering the effect of the coupling between both flap and lag motions and the extensional motion of rotating blades. Wu and Haug [19] used substructuring techniques to model the coupling between the axial and flexural displacements, but no quantitative study was given to determine the relation between the critical speed and the size of the substructure at which instability may occur. The centrifugal geometric stiffening effect has been also accounted for by considering a prestressed reference configuration of the flexible body [12, 18]. Garcia-Vallejo et al. [6, 7] considered the geometric stiffening effect of a rotating beam when using the floating frame of reference formulation and the absolute nodal coordinate formulation (ANCF) [3]. They introduced a new correction to the floating frame of reference formulation that leads to coupling between the bending and extension.

In most existing finite element beam models, the dimensions of the cross section are assumed to remain constant when the beam deforms. This, in fact, is the underlying assumption used in both Euler–Bernoulli and Timoshenko beam theories. In some of the finite element absolute nodal coordinate formulation beam models, this assumption is relaxed allowing the beam cross section dimensions to change. In the absolute nodal coordinate formulation, which allows for the use of general constitutive equations and strain-displacement relationships, several methods can be used to formulate the elastic forces. One method that has been used by several investigators is based on the general continuum mechanics approach. When the general continuum mechanics approach is used, the resulting new beam model leads to a geometric coupling between the deformation of the cross section and the beam axial and bending deformations. This kinematic coupling can be important in the case of very flexible structures and/or in some plasticity applications in order to realistically account for the change in the cross section dimensions when the structures deform. However, in the case of very stiff and thin structures, the resulting *ANCF coupled deformation modes* [9, 15] can have high frequencies that do not compare well with the analytical solution that is based on the assumption that the cross section dimensions do not change when the beam deforms. Nonetheless, using the absolute nodal coordinate formulation, one can still obtain the analytical eigenvalue solution by systematically eliminating the coupling between the

Journal ID: 11044, Article ID: 9070, Date: 2007-06-28, Proof No: 1

« MUBO 11044 layout: Small Condensed v.1.2 reference style: mathphys file: mubo9070.tex (Aiste) aid: 9070 doctopic: OriginalPaper class: spr-small-v1.1 v.2007/06/28 Prn:28/06/2007; 15:52 p. 3»

cross section deformation and the beam axial and bending deformation [15]. In this case, another method for formulating the elastic forces must be used. Two of these methods are considered in this study, which is focused on examining the effect of the centrifugal forces on the eigenvalue solution of rotating beams. In the first of these two methods, the *elastic line approach* is used; while in the second method, the elastic line approach is used with the *Hellinger–Reissner principle*. Multi-field principles are used often in the finite element literature to solve the locking problems.

It is the purpose of this study to examine the effect of the centrifugal forces on the finite element eigenvalue solution of rotating beams. The eigenvalue solution is obtained using two different nonlinear finite element formulations. The first formulation employs a geometrically exact beam model which assumes that the cross section does not deform in its own plane and remains plane after deformation, while the second formulation, the absolute nodal coordinate formulation, relaxes this assumption. Several ANCF beam models are used in this study. The first is based on a general continuum mechanics approach, the second is based on an elastic line approach, the third combines the elastic line approach with the Hellinger–Reissner principle, and the fourth is a general continuum mechanics based plate model for the beam. The centrifugal forces are formulated as function of the finite element nodal coordinates and the beam angular velocity. The resulting frequencies of the flap and lag modes are determined, and the solutions obtained using the two different nonlinear finite element formulations are compared. It is shown that when the ANCF coupled deformation modes are neglected [9, 15], the two solutions obtained using the two nonlinear formulations are in a very good agreement for different values of the beam angular velocity. It is important also to recognize that since the geometrically exact beam theory assumes that the beam cross section remains rigid, the two normal strain components associated with the cross section deformation are equal to zero; and as a consequence, Poisson ratio does not enter into the formulation of the elastic forces. It is shown in this investigation that when the effect of the Poisson ratio is neglected, the eigenvalue solution obtained using the absolute nodal coordinate formulation and the general continuum mechanics approach is in a good agreement with the solution obtained using the geometrically exact beam model. This paper is organized as follows. In Sect. 2, the geometrically exact beam formulation used in this study is briefly discussed. In Sect. 3, the formulation of the centrifugal forces based on the geometrically exact beam model is described. In Sect. 4, the four different finite element absolute nodal coordinate formulation beam models used in this study are presented. Section 5 describes the formulation of the centrifugal forces based on the absolute nodal coordinate formulation. In this section, the eigenvalue equations expressed in terms of the absolute nodal coordinates are also presented. In Sect. 6, numerical results are presented in order to examine the effect of the centrifugal forces on the eigenvalue solution of the rotating beam. The results obtained using the two nonlinear finite element formulations for the flap and lag modes are compared for different beam angular velocities. Summary and conclusions drawn from this study are presented in Sect. 7.

2 Geometrically exact beam theory

In this section and the following section, the geometrically exact finite element beam theory used in this investigation to formulate the centrifugal forces and study their effect on the eigenvalue solution is presented. More discussions on this formulation can be found in the literature [1]. Application of this formulation to rotorcraft problems was demonstrated by Bauchau et al. [2].

Journal ID: 11044, Article ID: 9070, Date: 2007-06-28, Proof No: 1

« MUBO 11044 layout: Small Condensed v.1.2 reference style: mathphys file: mubo9070.tex (Aiste) aid: 9070 doctopic: OriginalPaper class: spr-small-v1.1 v.2007/06/28 Prn:28/06/2007; 15:52 p. 4»

2.1 Kinematics of the problem

Consider a beam of length L with a cross section A of arbitrary shape, as depicted in Fig. 1. The volume of the beam is generated by sliding the cross section along the reference line of the beam, which is an arbitrary space curve. For this particular application, the reference line is selected to be coincident with the centerline of the beam. An inertial frame of reference $I = (\mathbf{i}_1, \mathbf{i}_2, \mathbf{i}_3)$ is used. Let $\mathbf{X}_0(\alpha_1)$ be the position vector of a point on the centerline of the beam in the reference configuration; α_1 is a curvilinear coordinate that measures length along the beam centerline. The position vector of a material point on the beam can be written as

$$\mathbf{X}(\alpha_1, \alpha_2, \alpha_3) = \mathbf{X}_0(\alpha_1) + \Delta\mathbf{X}(\alpha_1, \alpha_2, \alpha_3) \tag{1}$$

where $\Delta\mathbf{X} = \alpha_2\mathbf{E}_2(\alpha_1) + \alpha_3\mathbf{E}_3(\alpha_1)$. The vectors $\mathbf{E}_2$ and $\mathbf{E}_3$ define the plane of the cross section of the beam, and α_2 and α_3 are material coordinates along those axes. The coordinates α_1, α_2 and α_3 form a natural choice of coordinates (parameters) to represent the beam. Let the tangent to the centerline of the beam be $\mathbf{E}_1 = \partial\mathbf{X}_0/\partial\alpha_1$. Since the cross section is perpendicular to the centerline at the reference configuration, and $\mathbf{E}_2$ and $\mathbf{E}_3$ are chosen to be in the cross section plane and perpendicular to each other, the basis $B^0 = (\mathbf{E}_1, \mathbf{E}_2, \mathbf{E}_3)$ is orthonormal. This basis can be related to the inertial frame through a finite rotation tensor $\mathbf{R}_0$ such that $\mathbf{E}_i = \mathbf{R}_0\mathbf{i}_i$. The derivative of this basis along the axis of the beam is

$$\mathbf{R}_0^T\mathbf{E}_i' = \tilde{\mathbf{K}}\mathbf{i}_i \tag{2}$$

where $'$ indicates a derivative with respect to α_1, and $\tilde{\mathbf{K}} = \mathbf{R}_0^T\mathbf{R}_0'$ is the skew symmetric matrix associated with the curvature vector in the reference configuration. If $\mathbf{K} = [\,K_1 \quad K_2 \quad K_3\,]^T$ is the curvature vector, K_1 is the twist, or pretwist, of the beam, and K_2 and K_3 its natural curvatures. The base vectors in the reference configuration are $\mathbf{G}_i = \partial\mathbf{X}/\partial\alpha_i$ with $i = 1, 2, 3$, which can be written as

$$\mathbf{G}_1 = \mathbf{R}_0\big[\mathbf{i}_1 + \tilde{\mathbf{K}}(\alpha_2\mathbf{i}_2 + \alpha_3\mathbf{i}_3)\big], \qquad \mathbf{G}_2 = \mathbf{R}_0\mathbf{i}_2, \qquad \mathbf{G}_3 = \mathbf{R}_0\mathbf{i}_3. \tag{3}$$

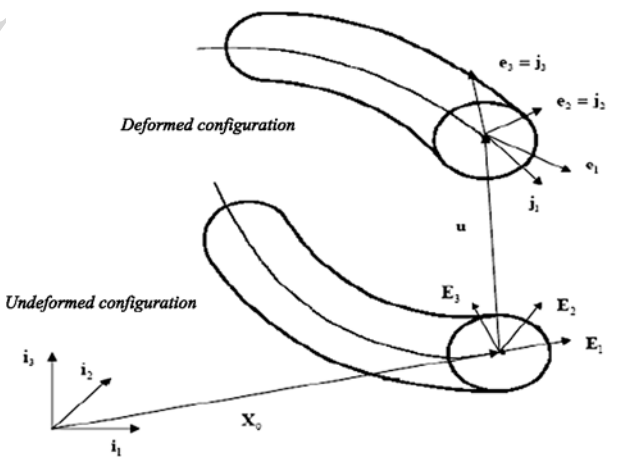

Fig. 1 Geometrically exact beam theory

Journal ID: 11044, Article ID: 9070, Date: 2007-06-28, Proof No: 1

« MUBO 11044 layout: Small Condensed v.1.2 reference style: mathphys file: mubo9070.tex (Aiste) aid: 9070 doctopic: OriginalPaper class: spr-small-v1.1 v.2007/06/28 Prn:28/06/2007; 15:52 p. 5»

The metric tensor of the reference configuration can be readily computed as

$$\mathbf{G} = \begin{bmatrix} (1-\alpha_2 K_3+\alpha_3 K_2)^2+(\alpha_3 K_1)^2+(\alpha_2 K_1)^2 & -\alpha_3 K_1 & \alpha_2 K_1 \\ -\alpha_3 K_1 & 1 & 0 \\ \alpha_2 K_1 & 0 & 1 \end{bmatrix} \tag{4}$$

where each of the terms is calculated using $G_{ij} = \mathbf{G}_i^T \mathbf{G}_j$ with $i, j = 1, 2, 3$.

In the deformed configuration of the beam, the position vector of a material point is written as

$$\mathbf{r}(\alpha_1, \alpha_2, \alpha_3) = \mathbf{r}_0(\alpha_1) + \Delta\mathbf{r}(\alpha_1, \alpha_2, \alpha_3) = \mathbf{X}_0(\alpha_1) + \mathbf{u}(\alpha_1) + \Delta\mathbf{r}(\alpha_1, \alpha_2, \alpha_3) \tag{5}$$

where $\mathbf{r}_0$ is the position of a material point on the centerline of the beam expressed as the sum of the position vector $\mathbf{X}_0$ of this point in the reference configuration and $\mathbf{u}$, the centerline displacement vector. $\Delta\mathbf{r}$ is now the position vector of a material point with respect to the centerline in the deformed configuration. The base vectors in the deformed configuration become $\mathbf{g}_i = \partial\mathbf{r}/\partial\alpha_i$, and at the centerline $\mathbf{e}_i = \mathbf{g}_i(\alpha_2 = \alpha_3 = 0)$, with $i = 1, 2, 3$. Two fundamental assumptions are made concerning the deformation of the beam: the cross section does not deform in its own plane, and the cross section remains plane after deformation. Note that the plane of the cross section is not assumed to remain normal to the centerline of the beam, allowing for transverse shearing deformations. These assumptions imply that each cross section displaces and rotates like a rigid body. Consequently, vectors $\mathbf{e}_2$ and $\mathbf{e}_3$ remain mutually orthogonal, unit vectors. An orthonormal basis $B = (\mathbf{j}_1, \mathbf{j}_2, \mathbf{j}_3)$ is defined as follows: $\mathbf{j}_2 = \mathbf{e}_2$, $\mathbf{j}_3 = \mathbf{e}_3$, $\mathbf{j}_1 = \mathbf{j}_2 \times \mathbf{j}_3$. Note that $\mathbf{e}_1$ is not a unit vector, nor is it orthogonal to $\mathbf{e}_2$ or $\mathbf{e}_3$, as axial and transverse shearing strains develop during deformation. Let $\mathbf{R}(\alpha_1)$ be the finite rotation tensor that brings basis B^0 to basis B, that is, $\mathbf{j}_1(\alpha_1) = \mathbf{R}(\alpha_1)\mathbf{E}_1 = \mathbf{R}\mathbf{R}_0\mathbf{i}_1$. Since the cross section remains rigid during the deformation process, the vector $\Delta\mathbf{r}$ must be entirely contained in the plane of the cross section in the deformed configuration. Hence,

$$\Delta\mathbf{r}(\alpha_1, \alpha_2, \alpha_3) = \alpha_2\mathbf{e}_2 + \alpha_3\mathbf{e}_3 = \alpha_2\mathbf{j}_2(\alpha_1) + \alpha_3\mathbf{j}_3(\alpha_1) = \mathbf{R}(\alpha_1)\Delta\mathbf{X} \tag{6}$$

which implies that during deformation, the relative position vector of all material points of a cross section undergo a rigid body rotation defined by the finite rotation tensor $\mathbf{R}$. The position vector of a material point in the deformed configuration can be written as

$$\mathbf{r}(\alpha_1, \alpha_2, \alpha_3) = \mathbf{X}_0(\alpha_1) + \mathbf{u}(\alpha_1) + \mathbf{R}(\alpha_1)\Delta\mathbf{X}(\alpha_1, \alpha_2, \alpha_3). \tag{7}$$

The base vectors in the deformed configuration can be readily obtained as $\mathbf{g}_1 = \mathbf{E}_1 + \mathbf{u}' + \alpha_2\mathbf{e}_2' + \alpha_3\mathbf{e}_3'$, $\mathbf{g}_2 = \mathbf{e}_2$ and $\mathbf{g}_3 = \mathbf{e}_3$; the corresponding base vectors at the centerline are then $\mathbf{e}_1 = \mathbf{E}_1 + \mathbf{u}'$, $\mathbf{e}_2 = \mathbf{j}_2$ and $\mathbf{e}_3 = \mathbf{j}_3$, respectively. The components of vectors $\mathbf{e}_1$, $\mathbf{e}_2$, and $\mathbf{e}_3$ can be expressed in the material system B as $\mathbf{e}_i^* = (\mathbf{R}\mathbf{R}_0)^T\mathbf{e}_i$, where * means that the vector is defined in the material coordinate system. The vector components $\mathbf{e}_1^*$, $\mathbf{e}_2^*$, and $\mathbf{e}_3^*$ are denoted

$$\mathbf{e}_1^* = [\,1+\bar{e}_{11} \quad 2\bar{e}_{12} \quad 2\bar{e}_{13}\,]^T, \qquad \mathbf{e}_2^* = [\,0 \quad 1 \quad 0\,]^T, \qquad \mathbf{e}_3^* = [\,0 \quad 0 \quad 1\,]^T \tag{8}$$

where $\bar{e}_{11}$, $\bar{e}_{12}$, and $\bar{e}_{13}$ are strain parameters. Vectors $\mathbf{e}_2^*$ and $\mathbf{e}_3^*$ are orthonormal due to the assumption that the cross section displaces and rotates like a rigid body. The components of vectors $\mathbf{e}_2'$ and $\mathbf{e}_3'$ can also be expressed in the material system, B, as $(\mathbf{e}_2')^* = (\mathbf{R}\mathbf{R}_0)^T\mathbf{e}_2' =$

Journal ID: 11044, Article ID: 9070, Date: 2007-06-28, Proof No: 1

« MUBO 11044 layout: Small Condensed v.1.2 reference style: mathphys file: mubo9070.tex (Aiste) aid: 9070 doctopic: OriginalPaper class: spr-small-v1.1 v.2007/06/28 Prn:28/06/2007; 15:52 p. 6»

$(\mathbf{RR}_0)^T\mathbf{j}_2' = \tilde{\mathbf{k}}\mathbf{i}_2$, $(\mathbf{e}_3')^* = (\mathbf{RR}_0)^T\mathbf{e}_3' = (\mathbf{RR}_0)^T\mathbf{j}_3' = \tilde{\mathbf{k}}\mathbf{i}_3$, where the components of the curvature are defined as the elements of the following matrix:

$$\tilde{\mathbf{k}} = (\mathbf{RR}_0)^T(\mathbf{RR}_0)' = \begin{bmatrix} 0 & -k_3 & k_2 \\ k_3 & 0 & -k_1 \\ -k_2 & k_1 & 0 \end{bmatrix}. \tag{9}$$

Next, the components of the base vectors in the deformed configuration are expressed in the material system B as $\mathbf{g}_i^* = (\mathbf{RR}_0)^T\mathbf{g}_i$, and their components are found as

$$\left.\begin{aligned} \mathbf{g}_1^* &= [\,1 + \bar{e}_{11} - \alpha_2 k_3 + \alpha_3 k_2 \quad 2\bar{e}_{12} - \alpha_3 k_1 \quad 2\bar{e}_{13} - \alpha_2 k_1\,]^T \\ \mathbf{g}_2^* &= [\,0 \quad 1 \quad 0\,]^T, \qquad \mathbf{g}_3^* = [\,0 \quad 0 \quad 1\,]^T \end{aligned}\right\}. \tag{10}$$

2.2 Strain analysis

The Green–Lagrange strain components ε_{ij} are defined as

$$\varepsilon_{ij} = \frac{1}{2}(g_{ij} - G_{ij}) \tag{11}$$

where $g_{ij} = \mathbf{g}_i^T\mathbf{g}_j$ is the metric tensor in the deformed configuration. The strain components are defined in the curvilinear coordinate system defined by the coordinates α_1, α_2, α_3. However, it is more convenient to work in a locally rectangular coordinate system defined by the basis B^0. The strain components expressed in these two systems are related by $\bar{\varepsilon}_{ij} = \varepsilon_{pq}\frac{\partial\alpha_p}{\partial\bar{\alpha}_i}\frac{\partial\alpha_q}{\partial\bar{\alpha}_j}$, where the rectangular coordinates along $\mathbf{E}_1$, $\mathbf{E}_2$, and $\mathbf{E}_3$ are denoted $\bar{\alpha}_1$, $\bar{\alpha}_2$ and $\bar{\alpha}_3$, respectively. It follows that

$$\frac{\partial\bar{\alpha}_i}{\partial\alpha_j} = \begin{bmatrix} \sqrt{G} & 0 & 0 \\ -\alpha_3 K_1 & 1 & 0 \\ \alpha_2 K_1 & 0 & 1 \end{bmatrix} \tag{12}$$

where $\sqrt{G} = (1 - \alpha_2 K_3 + \alpha_3 K_2)$ is the square root of the determinant of the metric tensor in the reference configuration. The strain components in the rectangular system become

$$\left.\begin{aligned} G\bar{\varepsilon}_{11} &= \varepsilon_{11} + 2\alpha_3 K_1\varepsilon_{12} - 2\alpha_2 K_1\varepsilon_{13} \\ \sqrt{G}\bar{\varepsilon}_{12} &= \varepsilon_{12}, \qquad \sqrt{G}\bar{\varepsilon}_{13} = \varepsilon_{13} \\ \bar{\varepsilon}_{22} &= \bar{\varepsilon}_{33} = \bar{\varepsilon}_{23} = 0 \end{aligned}\right\}. \tag{13}$$

The fact that the strains in the plane of the cross section vanish is a direct implication of assuming undeformable cross section.

The formulation presented in this section focuses on beams with a shallow curvature, that is, $\alpha_2 K_3 \ll 1$ and $\alpha_3 K_2 \ll 1$, which implies $\sqrt{G} \approx 1$. It is also assumed that the beam undergoes small deformations, that is, all the strain and curvature components are assumed to remain much smaller than unity: $\bar{e}_{11}$, $2\bar{e}_{12}$, $2\bar{e}_{13}$, $\alpha_2\kappa_1$, $\alpha_3\kappa_1$, $\alpha_3\kappa_2$ and $\alpha_2\kappa_3 \ll 1$, where $\kappa_i = k_i - K_i$ are the elastic curvatures. Using these assumptions together with (11), the strain components of (13) then become

$$\left.\begin{aligned} \bar{\varepsilon}_{11} &= \bar{e}_{11} - \alpha_2\kappa_3 + \alpha_3\kappa_2 \\ 2\bar{\varepsilon}_{12} &= 2\bar{e}_{12} - \alpha_3\kappa_1 \\ 2\bar{\varepsilon}_{13} &= 2\bar{e}_{13} + \alpha_2\kappa_1 \end{aligned}\right\}. \tag{14}$$

Journal ID: 11044, Article ID: 9070, Date: 2007-06-28, Proof No: 1

« MUBO 11044 layout: Small Condensed v.1.2 reference style: mathphys file: mubo9070.tex (Aiste) aid: 9070 doctopic: OriginalPaper class: spr-small-v1.1 v.2007/06/28 Prn:28/06/2007; 15:52 p. 7»

These equations can be written in a matrix form as follows

$$\bar{\boldsymbol{\varepsilon}} = \bar{\mathbf{e}} + \Delta\tilde{\mathbf{X}}^T\boldsymbol{\kappa} \tag{15}$$

where $\bar{\boldsymbol{\varepsilon}} = [\bar{\varepsilon}_{11}\ 2\bar{\varepsilon}_{12}\ 2\bar{\varepsilon}_{13}]^T$ and $\bar{\mathbf{e}} = [\bar{e}_{11}\ 2\bar{e}_{12}\ 2\bar{e}_{13}]^T$.

The reference curve strains are

$$[\,1+\bar{e}_{11}\quad 2\bar{e}_{12}\quad 2\bar{e}_{13}\,]^T = (\mathbf{R}\mathbf{R}_0)^T\mathbf{e}_1, \qquad \tilde{\boldsymbol{\kappa}} = \tilde{\mathbf{k}} - \tilde{\mathbf{K}} = \mathbf{R}_0^T\left(\mathbf{R}^T\mathbf{R}'\right)\mathbf{R}_0 - \mathbf{R}_0^T\mathbf{R}_0'. \tag{16}$$

The base vectors are $\mathbf{e}_1 = \mathbf{E}_1 + \mathbf{u}'$, $\mathbf{e}_2 = \mathbf{R}\mathbf{R}_0\mathbf{i}_2$ and $\mathbf{e}_3 = \mathbf{R}\mathbf{R}_0\mathbf{i}_3$. Equation (14) defines the strain-displacement relationships. The reference axis strains and curvatures are defined by (16). The strains are expressed in terms of six displacement components, three translational components, $\mathbf{u}$, and the three rotational components that define the finite rotation tensor $\mathbf{R}$.

3 Eigenvalue solution using the geometrically exact formulation

In this section, the governing equations of the rotating beam using the geometrically exact beam formulation and the constitutive laws are presented.

3.1 Governing equations

First, the governing equations for the static problem are presented. The principle of virtual work states

$$\int_0^L \int_A \delta\bar{\boldsymbol{\varepsilon}}^T\boldsymbol{\tau}^*\, dA\, d\alpha_1 = \delta W_{\text{ext}} \tag{17}$$

where $\boldsymbol{\tau}^* = [\tau_{11}^*\ \tau_{12}^*\ \tau_{13}^*]^T$ is the stress vector and $\delta\bar{\boldsymbol{\varepsilon}} = \delta\bar{\mathbf{e}} + \Delta\tilde{\mathbf{X}}^T\delta\boldsymbol{\kappa}$. After integration over the cross section of the beam, (17) becomes

$$\int_0^L \left(\delta\bar{\mathbf{e}}^T\mathbf{N}^* + \delta\boldsymbol{\kappa}^T\mathbf{M}^*\right) d\alpha_1 = \delta W_{\text{ext}} \tag{18}$$

where $\mathbf{N}^* = [N_1^*\ N_2^*\ N_3^*]^T = \int_A \boldsymbol{\tau}^*\, dA$ and $\mathbf{M}^* = [M_1^*\ M_2^*\ M_3^*]^T = \int_A \Delta\tilde{\mathbf{X}}\boldsymbol{\tau}^*\, dA$ are the axial and transverse forces, and the twisting and bending moments, respectively, measured in the material frame. Using (16), the variations in strain components can be expressed as

$$\delta\bar{\mathbf{e}} = (\mathbf{R}\mathbf{R}_0)^T\left(\delta\mathbf{u}' + \tilde{\mathbf{e}}_1^T\delta\boldsymbol{\psi}\right), \qquad \delta\boldsymbol{\kappa} = (\mathbf{R}\mathbf{R}_0)^T\delta\boldsymbol{\psi}' \tag{19}$$

where $\delta\tilde{\boldsymbol{\psi}} = \mathbf{R}^T\delta\mathbf{R}$ is the virtual rotation vector. The principle of virtual work becomes

$$\int_0^L \left[\left(\delta\mathbf{u}'^T + \delta\boldsymbol{\psi}^T\tilde{\mathbf{e}}_1\right)\mathbf{R}\mathbf{R}_0\mathbf{N}^* + \delta\boldsymbol{\psi}'^T\mathbf{R}\mathbf{R}_0\mathbf{M}^*\right] d\alpha_1 = \delta W_{\text{ext}}. \tag{20}$$

The beam internal forces and moments in the inertial system, $\mathbf{N} = \mathbf{R}\mathbf{R}_0\mathbf{N}^*$ and $\mathbf{M} = \mathbf{R}\mathbf{R}_0\mathbf{M}^*$, respectively, are defined. The virtual work of the external forces can be written as

$$\delta W_{\text{ext}} = \int_0^L \left(\delta\mathbf{u}^T\mathbf{F}_e + \delta\boldsymbol{\psi}^T\mathbf{M}_e\right) d\alpha_1 \tag{21}$$

Journal ID: 11044, Article ID: 9070, Date: 2007-06-28, Proof No: 1

« MUBO 11044 layout: Small Condensed v.1.2 reference style: mathphys file: mubo9070.tex (Aiste) aid: 9070 doctopic: OriginalPaper class: spr-small-v1.1 v.2007/06/28 Prn:28/06/2007; 15:52 p. 8»

where $\mathbf{F}_e$ and $\mathbf{M}_e$ are the external loads and moments on the beam per unit of length of the reference configuration. Integrating by parts and invoking the arbitrary nature of displacement variations yields the governing equations of the problem as

$$\mathbf{N}' = -\mathbf{F}_e, \qquad \mathbf{M}' + \tilde{\mathbf{e}}_1\mathbf{N} = -\mathbf{M}_e. \tag{22}$$

In the case of the dynamic problem, the inertia forces need to be introduced in the governing equations. In order to calculate the inertia forces, one needs to define the variation of kinetic energy. The inertial velocity $\mathbf{v}$ of a material point can be found by taking a time derivative of the inertial position vector defined in (7), to find $\mathbf{v} = \dot{\mathbf{u}} + \dot{\mathbf{R}}\Delta\mathbf{X}$. The components of the inertial velocity vector expressed in the material frame then become

$$\mathbf{v}^* = (\mathbf{R}\mathbf{R}_0)^T\mathbf{v} = (\mathbf{R}\mathbf{R}_0)^T\dot{\mathbf{u}} + (\mathbf{R}\mathbf{R}_0)^T\Delta\tilde{\mathbf{X}}^T\boldsymbol{\omega} \tag{23}$$

where $\boldsymbol{\omega}$ is the angular velocity. The two terms in (23) are associated with translation and rotation of the cross section respectively. Variations of the velocity components are then

$$\delta\left[(\mathbf{R}\mathbf{R}_0)^T\dot{\mathbf{u}}\right] = (\mathbf{R}\mathbf{R}_0)^T\left(\delta\dot{\mathbf{u}} + \tilde{\dot{\mathbf{u}}}^T\delta\boldsymbol{\psi}\right), \qquad \delta\left[(\mathbf{R}\mathbf{R}_0)^T\boldsymbol{\omega}\right] = (\mathbf{R}\mathbf{R}_0)^T\delta\dot{\boldsymbol{\psi}}. \tag{24}$$

The sectional velocities in the material system are

$$\boldsymbol{\upsilon}^* = \left[\,(\mathbf{R}\mathbf{R}_0)^T\dot{\mathbf{u}} \quad (\mathbf{R}\mathbf{R}_0)^T\boldsymbol{\omega}\,\right]^T. \tag{25}$$

The governing equations of motion of the problem are found with the help of Hamilton's principle as

$$\dot{\mathbf{H}} - \mathbf{N}' = \mathbf{F}_e, \qquad \dot{\mathbf{L}} + \tilde{\mathbf{u}}\mathbf{H} - \mathbf{M}' - \tilde{\mathbf{e}}_1\mathbf{N} = \mathbf{M}_e \tag{26}$$

where $\mathbf{H}$ and $\mathbf{L}$ are the sectional linear momentum and angular momentum, respectively.

3.2 Constitutive equations

To complete the formulation, the constitutive laws of the beam must be specified. First, the stiffness characteristics of the section are defined by the following relationship written in the material frame:

$$[\,\tilde{\boldsymbol{\varepsilon}} \quad \boldsymbol{\kappa}\,]^T = \mathbf{C}^*\left[\mathbf{N}^* \quad \mathbf{M}^*\right]^T \tag{27}$$

where $\mathbf{C}^*$ is the fully populated, 6×6 stiffness matrix of the section. This matrix can be obtained from the variational asymptotic procedure described by Hodges [8] and Cesnik et al. [4]. This approach provides a rigorous proof of the fact that the original three-dimensional elasticity problem splits into two independent problems: a linear, two-dimensional analysis of the cross section of the beam, and a nonlinear, one-dimensional problem along the axis of the beam. The first problem takes into account the three-dimensional nature of the beam deformation and includes a full finite element discretization of the section, which can handle beam of arbitrary cross section made of anisotropic materials. The material frame defined in the preceding section is, in fact, a floating frame of reference for which the average warping vanishes. This removes the kinematic assumption stated above. The second, one-dimensional problem along the axis of the beam is identical to the geometrically exact formulation described above. The variational asymptotic approach to the problem guarantees the convergence of the results to those of three-dimensional elasticity.

Journal ID: 11044, Article ID: 9070, Date: 2007-06-28, Proof No: 1

« MUBO 11044 layout: Small Condensed v.1.2 reference style: mathphys file: mubo9070.tex (Aiste) aid: 9070 doctopic: OriginalPaper class: spr-small-v1.1 v.2007/06/28 Prn:28/06/2007; 15:52 p. 9»

The inertial constitutive laws relate the sectional linear momentum and angular momentum to the sectional velocities,

$$\begin{bmatrix} \mathbf{H}^* & \mathbf{L}^* \end{bmatrix}^T = \boldsymbol{\mu}^* \boldsymbol{\upsilon}^*. \tag{28}$$

The sectional mass matrix in the material system is

$$\boldsymbol{\mu}^* = \begin{bmatrix} m & m\tilde{\boldsymbol{\eta}}^{*T} \\ m\tilde{\boldsymbol{\eta}}^* & \mathbf{I}_0^* \end{bmatrix} \tag{29}$$

where m is the mass of the beam per unit span, $\boldsymbol{\eta}^*$ the components of position vector of the center of mass of the section with respect to the reference line of the beam, and $\mathbf{I}_0^*$ the components of the sectional mass moment of inertial tensor. Both $\boldsymbol{\eta}^*$ and $\mathbf{I}_0^*$ are measured in the material frame.

3.3 Determination of natural frequencies

To determine the natural frequencies of a rotating structure, a two-step procedure is followed. First, the static equilibrium configuration of the beam under the steady centrifugal forces associated with the rotation of the beam is computed. Next, the equations of motion of the system are linearized about this equilibrium configuration to obtain the linearized mass and stiffness matrices, which, in turns, form a generalized eigenvalue problem for the evaluation of the natural frequencies and associated mode shapes.

4 Absolute nodal coordinate formulation models

As previously mentioned, the goal of this study is to compare between the eigenvalue results obtained using the geometrically exact beam theory and the absolute nodal coordinate formulation when the effect of the centrifugal forces is considered. In this section, the different finite element absolute nodal coordinate formulation models used in this study are reviewed. Beam and plate finite element models are considered. While for the plate element model, only the general continuum mechanics approach is used to formulate the elastic forces, several models are used with the beam element. Specifically, three different beam models are considered; the first is based on the general continuum mechanics approach [16, 17, 20], the second is based on the elastic line approach [15, 17], while the third combines the elastic line approach and the Hellinger–Reissner principle [15]. In this section, the beam element with the three elastic force models is first presented, followed by the plate element model that employs the continuum mechanics to formulate the elastic forces [11].

In the absolute nodal coordinate formulation, the global position vector $\mathbf{r}$ of an arbitrary point on the finite element (beam or plate) can be defined using the element shape functions and the nodal coordinate vector as follows:

$$\mathbf{r} = \mathbf{S}(x, y, z)\mathbf{e} \tag{30}$$

where $\mathbf{S}$ is the element shape function matrix expressed in terms of the element spatial coordinates x, y, and z; and $\mathbf{e}$ is the vector of nodal coordinates that consist of absolute nodal position coordinates and position coordinate gradients. The element shape function used in (30) for the beam and plate elements used in this study are presented in Appendix 1. The use

Journal ID: 11044, Article ID: 9070, Date: 2007-06-28, Proof No: 1

« MUBO 11044 layout: Small Condensed v.1.2 reference style: mathphys file: mubo9070.tex (Aiste) aid: 9070 doctopic: OriginalPaper class: spr-small-v1.1 v.2007/06/28 Prn:28/06/2007; 15:52 p. 10»

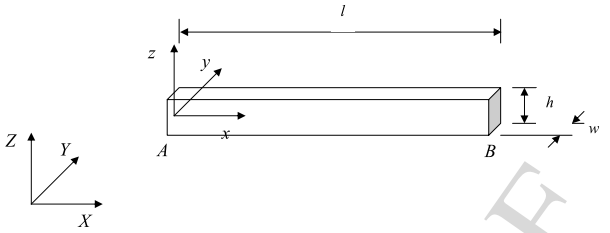

Fig. 2 Absolute nodal coordinate formulation beam model

of the representation in (30) leads to a constant mass matrix and zero Coriolis and centrifugal forces associated with the absolute nodal coordinates. In order to compare the ANCF eigenvalue solution with the results obtained using the geometrically exact beam model, the equations of motion are defined in a rotating coordinate system, leading to nonzero centrifugal forces.

4.1 Beam element formulation

Figure 2 shows the global and local coordinate systems used to define the absolute position and gradient coordinates for the three-dimensional beam element. The element nodal coordinate vector at node n is defined as follows:

$$\mathbf{e}^n = \left[\mathbf{r}^{nT} \quad \left(\frac{\partial \mathbf{r}^n}{\partial x}\right)^T \quad \left(\frac{\partial \mathbf{r}^n}{\partial y}\right)^T \quad \left(\frac{\partial \mathbf{r}^n}{\partial z}\right)^T \right]^T. \tag{31}$$

The vector of the element nodal coordinates can be written as follows:

$$\mathbf{e} = \left[\mathbf{e}^{A^T} \quad \mathbf{e}^{B^T} \right]^T. \tag{32}$$

This element has 24 degrees of freedom; 12 degrees of freedom per node.

Continuum mechanics approach In the general continuum mechanics approach [20], the elastic forces are formulated using the Green–Lagrange strain tensor defined as

$$\boldsymbol{\varepsilon}_m = \frac{1}{2}\left(\mathbf{J}^T\mathbf{J} - \mathbf{I}\right) \tag{33}$$

where $\mathbf{J}$ is the matrix of the position vector gradients, and $\mathbf{I}$ is the identity matrix. Using the principle of virtual work, the vector of generalized elastic forces $\mathbf{Q}^e$ is defined as

$$\mathbf{Q}^e = -\int_V \left(\frac{\partial \boldsymbol{\varepsilon}}{\partial \mathbf{e}}\right)^T \mathbf{E}\boldsymbol{\varepsilon}\, dV \tag{34}$$

where $\boldsymbol{\varepsilon}$ is a vector that consist of the six independent Green–Lagrange strain components, and $\mathbf{E}$ is the matrix of elastic coefficients [5]. The use of the continuum mechanics approach to formulate the elastic forces leads to a model that includes the ANCF coupled deformation modes [9, 15]. While these modes, as previously mentioned, can be important in very flexible structures and plasticity applications, for stiff and thin beams, the ANCF coupled deformation modes can have very high frequencies that do not compare well with the analytical solutions that are obtained based on the small deformation assumptions and the assumption of the rigidity of the cross section.

Journal ID: 11044, Article ID: 9070, Date: 2007-06-28, Proof No: 1

Elastic line approach In the elastic line approach [15], all the deformation modes are defined along the beam centerline. The slopes on the centerline are defined as

$$\mathbf{r}_x = \mathbf{r}_{,x}(x,0,0), \qquad \mathbf{r}_y = \mathbf{r}_{,y}(x,0,0), \qquad \mathbf{r}_z = \mathbf{r}_{,z}(x,0,0) \tag{35}$$

where $\mathbf{r}_{,\alpha} = \partial\mathbf{r}/\partial\alpha$ with $\alpha = x, y, z$. The strains and curvatures used in this model to formulate the elastic forces are defined as

$$\left.\begin{aligned} &\varepsilon_x = \frac{1}{2}\left(\mathbf{r}_x^T\mathbf{r}_x - 1\right), \qquad \varepsilon_y = \frac{1}{2}\left(\mathbf{r}_y^T\mathbf{r}_y - 1\right), \qquad \varepsilon_z = \frac{1}{2}\left(\mathbf{r}_z^T\mathbf{r}_z - 1\right),\\ &\gamma_{yz} = \mathbf{r}_y^T\mathbf{r}_z, \qquad \gamma_{xy} = \mathbf{r}_x^T\mathbf{r}_y, \qquad \gamma_{xz} = \mathbf{r}_x^T\mathbf{r}_z,\\ &\kappa_x = \frac{1}{2}\left(\mathbf{r}_z^T\mathbf{r}_{xy} - \mathbf{r}_y^T\mathbf{r}_{xz}\right), \qquad \kappa_y = \mathbf{r}_z^T\mathbf{r}_{xx}, \qquad \kappa_z = \mathbf{r}_y^T\mathbf{r}_{xx} \end{aligned}\right\} \tag{36}$$

where $\mathbf{r}_{xx} = \mathbf{r}_{,xx}(x,0,0)$.

In the elastic line approach, the total strain energy of the beam element W^e can be written as the sum of four different strain energy terms as follows:

$$W^e = W_c + W_s + W_b + W_t \tag{37}$$

where subscripts c, s, b and t refer, respectively, to extension and shear strain based on the definition of the vectors given in (35), shear strain, bending strain and torsion strain. These strain energy terms are calculated as follows [15]:

$$\left.\begin{aligned} &W_c = \frac{1}{2}\int_0^l A\bar{\boldsymbol{\varepsilon}}^T\bar{\mathbf{E}}\bar{\boldsymbol{\varepsilon}}\,dx, \qquad W_s = \frac{1}{2}\int_0^l A(Gk_y\gamma_{xy} + Gk_z\gamma_{xz})\,dx\\ &W_b = \frac{1}{2}\int_0^l E\left(I_y\kappa_y^2 + I_z\kappa_z^2\right)dx, \qquad W_t = \frac{1}{2}\int_0^l k_xGI_p\kappa_x\,dx \end{aligned}\right\} \tag{38}$$

where the integration is carried over the original length since small deformation assumptions are used in this paper, and

$$\bar{\boldsymbol{\varepsilon}} = (\varepsilon_x, \varepsilon_y, \varepsilon_z, \gamma_{yz})^T, \qquad \bar{\mathbf{E}} = \frac{2G}{(1-2\nu)}\begin{bmatrix} 1-\nu & \nu & \nu & 0\\ \nu & 1-\nu & \nu & 0\\ \nu & \nu & 1-\nu & 0\\ 0 & 0 & 0 & \frac{(1-2\nu)}{2} \end{bmatrix}. \tag{39}$$

In these expressions, l is the beam element length in the reference configuration, E is the modulus of elasticity, G is the modulus of rigidity, ν is the Poisson ratio, A is the cross section area, I_y and I_z are the second moments of area, I_p is the polar moment of area, and k_x, k_y, and k_z are shear factors. In the case of the elastic line approach, the vector of generalized elastic forces $\mathbf{Q}^e$ is defined as:

$$\mathbf{Q}^e = -\frac{\partial W^e}{\partial \mathbf{e}}. \tag{40}$$

In the elastic line approach, the geometric coupling between the cross section and bending deformations is not considered in the formulation of the elastic forces. Consequently, a beam model based on this approach does not include the ANCF coupled deformation modes.

« MUBO 11044 layout: Small Condensed v.1.2 reference style: mathphys file: mubo9070.tex (Aiste) aid: 9070 doctopic: OriginalPaper class: spr-small-v1.1 v.2007/06/28 Prn:28/06/2007; 15:52 p. 12»

Elastic line approach/Hellinger–Reissner principle Multi-field variational principles are frequently used in the finite element literature to solve different locking problems, including volumetric, shear and membrane locking. In this section, as an example, the Hellinger–Reissner principle is used. In this principle, independent interpolation is made for the transverse shear stresses [13]. One can assume that the shear stresses will vary linearly over the elastic line of the element [15]. Both shear stresses τ_{xy} and τ_{xz} can be interpolated independent of the displacement field interpolation. For example, consider the τ_{xy} component. This shear strain component can be assumed in the following form:

$$\tau_{xy} = \mathbf{N}\boldsymbol{\tau}^*_{xy} \tag{41}$$

where $\mathbf{N}$ is an assumed shape function matrix, and $\boldsymbol{\tau}^*_{xy}$ is a vector of shear stresses that can be determined using the Hellinger–Reissner principle. Schwab and Meijaard [15] assumed a linear interpolation in (41). In this case, the shape function matrix is given by

$$\mathbf{N} = [\,1-\xi \quad \xi\,] \tag{42}$$

where $\xi = x/l$. Using this linear interpolation, the vector of shear stresses $\boldsymbol{\tau}^*_{xy}$ has two elements and can be defined as

$$\boldsymbol{\tau}^*_{xy} = \left[\,\tau^A_{xy} \quad \tau^B_{xy}\,\right]^T \tag{43}$$

where $\tau^A_{xy} = \tau_{xy}$ $(\xi = 0)$ and $\tau^B_{xy} = \tau_{xy}$ $(\xi = 1)$. Using the Hellinger–Reissner principle, the strain energy associated with the shear strain in the xy-plane can be written as

$$W^*_{xy} = \int_V \left(\tau_{xy}\gamma_{xy} - W^c_{xy}(\tau_{xy})\right) dV. \tag{44}$$

In this equation, γ_{xy} is as defined in terms of the nodal coordinates using (36), and W^c_{xy} is the complementary shear stress energy which is defined by the equation

$$W^c_{xy}(\tau_{xy}) = \frac{1}{2Gk_y}(\tau_{xy})^2. \tag{45}$$

Substituting (41) and (45) into (44), we obtain

$$W^*_{xy} = \int_V \left(\boldsymbol{\tau}^{*T}_{xy}\mathbf{N}^T\gamma_{xy} - \frac{1}{2Gk_y}\boldsymbol{\tau}^{*T}_{xy}\mathbf{N}^T\mathbf{N}\boldsymbol{\tau}^*_{xy}\right) dV. \tag{46}$$

By minimizing this strain energy with respect to $\boldsymbol{\tau}^*_{xy}$, the stress vector $\boldsymbol{\tau}^*_{xy}$ can be determined in terms of γ_{xy}. In a similar manner $\boldsymbol{\tau}^*_{xz}$ can be determined. Using these vectors, the shear stresses τ_{xy} and τ_{xz} can be interpolated and used in the definition of the total strain energy function which can be used to define the elastic forces as previously described in this section. It is important to point out that the Hellinger–Reissner principle is a stress based variational principle. Multi-field (mixed) strain based variational principles are also frequently used in the finite element literature to deal with the locking problems.

4.2 Plate element model

Figure 3 shows the global and local coordinates used to define the absolute position and gradient coordinates for this element. The element nodal coordinate vector at node n is

Journal ID: 11044, Article ID: 9070, Date: 2007-06-28, Proof No: 1

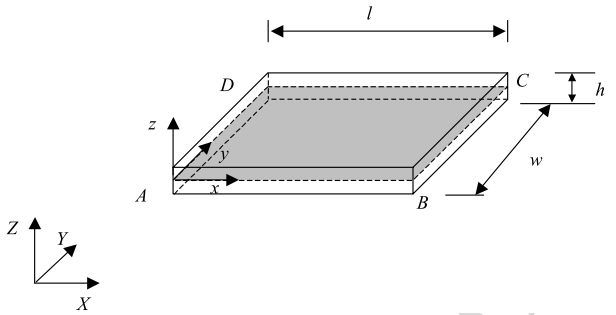

Fig. 3 Absolute nodal coordinate formulation plate model

defined as follows [11]:

$$\mathbf{e}^n = \left[\mathbf{r}^{nT} \quad \left(\frac{\partial \mathbf{r}^n}{\partial x}\right)^T \quad \left(\frac{\partial \mathbf{r}^n}{\partial y}\right)^T \quad \left(\frac{\partial \mathbf{r}^n}{\partial z}\right)^T \right]^T. \tag{47}$$

The vector of the element nodal coordinates can be written as follows:

$$\mathbf{e} = \left[\mathbf{e}^{AT} \quad \mathbf{e}^{BT} \quad \mathbf{e}^{CT} \quad \mathbf{e}^{DT} \right]^T. \tag{48}$$

This element has 48 degrees of freedom; 12 degrees of freedom per node. Using the general continuum mechanics approach, the elastic forces can be formulated using (33) and (34); by following a procedure similar to the one used for the beam element. Therefore, this plate element model also includes the ANCF coupled deformation modes. The plate element shape function matrix used in this investigation is presented in Appendix 1 of this paper.

5 Formulation of the ANCF centrifugal forces

In this section, the method used in this investigation to study the effect of the centrifugal forces on the eigenvalue solution when using the absolute nodal coordinate formulation (ANCF) is presented. Recall that the mass matrix obtained using the absolute nodal coordinate formulation is constant, and as a result, the centrifugal and Coriolis forces are equal to zero. If a frame that rotates with the beam is used to define the coordinates instead of the inertial frame, the resulting equations will include centrifugal forces as will be demonstrated in this section. These forces can then be expressed in terms of the beam specified constant angular velocity.

The equation of motion of the rotating beam formulated using the absolute nodal coordinate formulation can be written as

$$\mathbf{M}\ddot{\mathbf{e}} + \mathbf{Q}_e = \mathbf{Q}_r \tag{49}$$

where $\mathbf{M}$ is the constant symmetric mass matrix, $\ddot{\mathbf{e}}$ is the vector of nodal accelerations, $\mathbf{Q}_e$ is the vector of generalized elastic forces, and $\mathbf{Q}_r$ is the vector of the constraint forces. In order to write the equations of motion in terms of coordinates defined with respect to the rotating frame, the absolute coordinates need to be expressed in terms of the new set of coordinates. Assuming that the first node of the beam does not translate, the following coordinate transformation can be developed:

$$\mathbf{e} = \mathbf{A}\mathbf{q} \tag{50}$$

Journal ID: 11044, Article ID: 9070, Date: 2007-06-28, Proof No: 1

where $\mathbf{q}$ is the vector of absolute coordinates defined in the rotating frame, and the matrix $\mathbf{A}$ is the coordinate transformation matrix. In this study, a simple rotation of the beam about a fixed axis is considered. In this case, without any loss of generality, the matrix $\mathbf{A}$ can be written in the case of the absolute nodal coordinate formulation as

$$\mathbf{A} = \begin{bmatrix} \mathbf{A}_0 & \mathbf{0} & \dots & \mathbf{0} \\ \mathbf{0} & \mathbf{A}_0 & \dots & \mathbf{0} \\ \vdots & \vdots & \ddots & \vdots \\ \mathbf{0} & \mathbf{0} & \dots & \mathbf{A}_0 \end{bmatrix} \tag{51}$$

where $\mathbf{A}$ has dimension equal to the total number of nodal coordinates, and $\mathbf{A}_0$ is a 3×3 orthogonal matrix defined as

$$\mathbf{A}_0 = \begin{bmatrix} \cos\theta & -\sin\theta & 0 \\ \sin\theta & \cos\theta & 0 \\ 0 & 0 & 1 \end{bmatrix} \tag{52}$$

where θ is the angle of rotation about the fixed axis of rotation. Note that both matrices $\mathbf{A}$ and $\mathbf{A}_0$ are orthogonal matrices.

Differentiating (50) twice with respect to time, substituting the result into (49), and pre-multiplying by $\mathbf{A}^T$, the equations of motion in the rotating frame can be written as

$$\mathbf{A}^T\mathbf{M}\mathbf{A}\ddot{\mathbf{q}} + 2\mathbf{A}^T\mathbf{M}\dot{\mathbf{A}}\dot{\mathbf{q}} + \mathbf{A}^T\mathbf{M}\ddot{\mathbf{A}}\mathbf{q} + \mathbf{A}^T\mathbf{Q}_e = \mathbf{A}^T\mathbf{Q}_r \tag{53}$$

where the matrices $\dot{\mathbf{A}}$ and $\ddot{\mathbf{A}}$ are presented in Appendix 2. In the rotating beam model used in the comparative numerical study presented in this investigation, simple linear constraints are imposed on the absolute coordinates $\mathbf{q}$, as will be discussed in the following section. Using these simple constraint equations, the vector of coordinates $\mathbf{q}$ can be written in terms of a selected set of independents coordinates $\mathbf{q}_i$ as follows:

$$\mathbf{q} = \mathbf{B}\mathbf{q}_i + \boldsymbol{\gamma} \tag{54}$$

where $\mathbf{B}$ and $\boldsymbol{\gamma}$ are constant in the application considered in this paper. Substituting this equation into (53), one obtains the equations of motion of the system expressed in terms of independent coordinates defined in the rotating frame. These equations can be written as:

$$\hat{\mathbf{M}}\ddot{\mathbf{q}}_i + \hat{\mathbf{C}}\dot{\mathbf{q}}_i + \hat{\mathbf{K}}\mathbf{q}_i + \hat{\mathbf{Q}}_\gamma + \hat{\mathbf{Q}}_e = \mathbf{0} \tag{55}$$

where

$$\left.\begin{aligned} \hat{\mathbf{M}} &= \mathbf{B}^T\mathbf{A}^T\mathbf{M}\mathbf{A}\mathbf{B}, & \hat{\mathbf{C}} &= 2\mathbf{B}^T\mathbf{A}^T\mathbf{M}\dot{\mathbf{A}}\mathbf{B}, \\ \hat{\mathbf{K}} &= \mathbf{B}^T\mathbf{A}^T\mathbf{M}\ddot{\mathbf{A}}\mathbf{B}, & \hat{\mathbf{Q}}_\gamma &= \mathbf{B}^T\mathbf{A}^T\mathbf{M}\ddot{\mathbf{A}}\mathbf{B}\gamma \\ \hat{\mathbf{Q}}_e &= \mathbf{B}^T\mathbf{A}^T\mathbf{Q}_e \end{aligned}\right\}. \tag{56}$$

Since the equations of motion are expressed in terms of the independents coordinates, the constraint forces are automatically eliminated.

As pointed out by Garcia-Vallejo et al. [7], the forms of the mass matrix and the elastic forces in the absolute nodal coordinate formulation do not change under an orthogonal coordinate transformation. That is, $\mathbf{A}^T\mathbf{M}\mathbf{A} = \mathbf{M}$ for any orthogonal matrix $\mathbf{A}$. It follows that the first matrix in (56) reduces to $\hat{\mathbf{M}} = \mathbf{B}^T\mathbf{M}\mathbf{B}$. While the transformation matrix $\mathbf{A}$ and its derivatives appear in other components of (56), one can also show that the matrices and

« MUBO 11044 layout: Small Condensed v.1.2 reference style: mathphys file: mubo9070.tex (Aiste) aid: 9070 doctopic: OriginalPaper class: spr-small-v1.1 v.2007/06/28 Prn:28/06/2007; 15:52 p. 15»

vectors that appear in this equation do not depend on the angle of rotation θ. To this end, the following identities can be used:

$$\mathbf{A}_0^T\mathbf{A}_0 = \mathbf{I}, \qquad \mathbf{A}_0^T\mathbf{A}_{0\theta} = \tilde{\mathbf{I}}, \qquad \mathbf{A}_{0\theta\theta} = -\mathbf{A}_{0r} \tag{57}$$

where $\mathbf{A}_0$ is defined in (52), and

$$\mathbf{A}_{0\theta} = \frac{\partial \mathbf{A}_0}{\partial \theta}, \qquad \tilde{\mathbf{I}} = \begin{bmatrix} 0 & -1 & 0 \\ 1 & 0 & 0 \\ 0 & 0 & 0 \end{bmatrix}, \qquad \mathbf{A}_{0r} = \begin{bmatrix} \cos\theta & -\sin\theta & 0 \\ \sin\theta & \cos\theta & 0 \\ 0 & 0 & 0 \end{bmatrix}. \tag{58}$$

Utilizing these identities and using the fact that the element shape function in the absolute nodal coordinate formulation can always be written in the following form:

$$\mathbf{S} = [\, S_1\mathbf{I} \quad S_2\mathbf{I} \quad \ldots \quad S_m\mathbf{I} \,], \tag{59}$$

one can show, as demonstrated in Appendix 2, that the matrices and vectors that appear in (56) do not depend on the angle θ that defines the orientation of the rotating frame with respect to the inertial frame. This important fact will be utilized in the development presented in the remainder of this study.

The goal in this study, as previously mentioned, is to examine the effect of the centrifugal forces on the eigenvalue solution of the rotating beam about an equilibrium position. To this end, the static equilibrium position coordinates $\mathbf{q}_{is}$ are first determined for a given specified constant value of the angular velocity. Other velocity and acceleration coordinates are assumed to be zero. Using $\mathbf{q}_{is}$ to define the position coordinates in the equations of motion, one can formulate an eigenvalue problem, which can be solved for the flap and lag modes of the rotating beam.

5.1 Static equilibrium

In the static equilibrium analysis presented in this section, the effect of the gravity forces is neglected, and the static configuration due to the effect of the centrifugal forces is determined. As previously discussed in this section, the matrices that appear in the equations of motion of the rotating beam obtained using the absolute nodal coordinate formulation do not depend on the angle that defines the orientation of the rotating frame with respect to the inertial frame. Consequently, the static equilibrium configuration $\mathbf{q}_{is}$ of the model used in this investigation does not depend on the orientation angle θ. In the case of the static analysis, $\ddot{\mathbf{q}}_{is} = \dot{\mathbf{q}}_{is} = \mathbf{0}$, which upon the use of (55) becomes

$$\hat{\mathbf{K}}\mathbf{q}_{is} + \hat{\mathbf{Q}}_\gamma + \hat{\mathbf{Q}}_e(\mathbf{q}_{is}) = \mathbf{0}. \tag{60}$$

This is a nonlinear system of equations that can be solved numerically using a Newton–Raphson algorithm to determine $\mathbf{q}_{is}$. In the preceding equation, the stiffness matrix $\hat{\mathbf{K}}$ and the centrifugal force vector $\hat{\mathbf{Q}}_\gamma$ depend on the prescribed angular velocity, which is assumed to be constant.

5.2 Eigenvalue analysis

In order to obtain the solution of the eigenvalue problem of the rotating beam including the effect of the centrifugal forces, the equations of motion at a particular static configuration $\mathbf{q}_{is}$

Journal ID: 11044, Article ID: 9070, Date: 2007-06-28, Proof No: 1

« MUBO 11044 layout: Small Condensed v.1.2 reference style: mathphys file: mubo9070.tex (Aiste) aid: 9070 doctopic: OriginalPaper class: spr-small-v1.1 v.2007/06/28 Prn:28/06/2007; 15:52 p. 16»

and a prescribed angular velocity $\omega_0 = \dot{\theta}$ are linearized. The linearized equations of motion used in this investigation to perform the eigenvalue analysis are

$$\hat{\mathbf{M}}\ddot{\mathbf{q}}_i + \hat{\mathbf{C}}\dot{\mathbf{q}}_i + \hat{\mathbf{K}}^*\mathbf{q}_i = \mathbf{0} \tag{61}$$

where

$$\hat{\mathbf{K}}^* = \hat{\mathbf{K}} + \mathbf{B}^T\mathbf{A}^T\frac{\partial \mathbf{Q}_e}{\partial \mathbf{q}_i}(\mathbf{q}_{is}). \tag{62}$$

Note that in (61), there is a damping term. The effect of this damping term on the computed eigenvalues was found to be significant. It is also important to mention before concluding this section that the procedure used for formulating the eigenvalue problem based on the absolute nodal coordinate formulation is consistent with the procedure used in the geometrically exact beam theory previously discussed in this investigation.

6 Numerical results

In this section, the results obtained for the eigenvalue analysis of the rotating cantilever beam using different nonlinear finite element absolute nodal coordinate formulations are presented and compared with the results obtained using the geometrically exact beam model. The dimensions and material properties of the beam are presented in Table 1. The results are obtained in this study assuming that the beam is rotating with an angular velocity of $0.1\omega_0, 0.2\omega_0, 0.3\omega_0, \ldots, \omega_0$, where the value of ω_0 is presented in Table 1. The main goal of this comparison is to show that when the effect of the ANCF coupled deformation modes is neglected, the eigenvalue solutions obtained using the geometrically exact beam theory and the absolute nodal coordinate formulation are in good agreement when the effect of the centrifugal forces of the rotating beam is taken into consideration in the linearized equations.

In the case of the beam model based on the ANCF, the degrees of freedom that are constrained at the first node are:

$$\mathbf{r}, \qquad \mathbf{r}_y|_x, \qquad \mathbf{r}_y|_z, \qquad \mathbf{r}_z|_x \tag{63}$$

where $\mathbf{x}|_\alpha$ indicates the α-th component of vector $\mathbf{x}$, with $\alpha = x, y, z$. Note that the resulting simple constraints used in this model can be written in the form of (54). In the case of the plate model based on the ANCF, the same constraints as in (63) are used for the two nodes fixed at the base. The total number of elements used for the beam and plate models is ten. Therefore, the total number of degrees of freedom of the system is 126 and 252 for the beam and plate models, respectively. In the case of the geometrically exact formulation, the

Table 1 Properties of the rotating beam

Parameter	Symbol	Value	Units
Density	ρ	2699.23	(kg/m^3)
Young modulus	E	727777×10^5	(N/m^2)
Poisson ratio	ν	0.3	–
Beam length	L	8.178698	(m)
Beam width	w	0.33528	(m)
Beam height	h	0.033528	(m)
Angular velocity	ω_0	27.02	(rad/s)

Journal ID: 11044, Article ID: 9070, Date: 2007-06-28, Proof No: 1

Table 2 Eigenfrequencies for the first flap mode at different angular velocities

Angular Veloc.	Geometrically exact beam model	ANCF_beam (continuum mechanic approach)	ANCF_beam (elastic line approach)	ANCF_beam (elastic line + Hellinger–Reissner) approach	ANCF_plate (continuum mechanic approach)
$0.0 * \omega_0$	2.64	3.07	2.64	2.64	2.83
$0.1 * \omega_0$	3.95	4.25	3.95	4.05	4.09
$0.2 * \omega_0$	6.37	6.59	6.38	6.44	6.49
$0.3 * \omega_0$	9.00	9.19	9.02	9.06	9.12
$0.4 * \omega_0$	11.67	11.86	11.71	11.73	11.81
$0.5 * \omega_0$	14.35	14.55	14.41	14.43	14.51
$0.6 * \omega_0$	17.04	17.26	17.12	17.16	17.22
$0.7 * \omega_0$	19.74	19.98	19.85	19.88	19.94
$0.8 * \omega_0$	22.44	22.70	22.57	22.61	22.67
$0.9 * \omega_0$	25.13	25.42	25.30	25.34	25.40
$1.0 * \omega_0$	27.83	28.15	28.03	28.05	28.13

Table 3 Eigenfrequencies for the second flap mode at different angular velocities

Angular Veloc.	Geometrically exact beam mode	ANCF_beam (continuum mechanic approach)	ANCF_beam (elastic line approach)	ANCF_beam (elastic line + Hellinger–Reissner approach)	ANCF_plate (continuum mechanic approach)
$0.0 * \omega_0$	16.55	19.46	16.76	16.61	17.97
$0.1 * \omega_0$	17.92	20.65	18.13	18.30	19.25
$0.2 * \omega_0$	21.52	23.86	21.71	21.86	22.66
$0.3 * \omega_0$	26.42	28.40	26.62	26.73	27.40
$0.4 * \omega_0$	32.01	33.73	32.22	32.33	32.89
$0.5 * \omega_0$	37.96	39.51	38.21	38.30	38.77
$0.6 * \omega_0$	44.12	45.56	44.41	44.55	44.89
$0.7 * \omega_0$	50.40	51.78	50.74	50.86	51.16
$0.8 * \omega_0$	56.76	58.11	57.16	57.33	57.51
$0.9 * \omega_0$	63.17	65.51	63.64	63.80	63.94
$1.0 * \omega_0$	69.62	70.98	70.17	70.22	70.41

model has 72 degrees of freedom. It was observed that if the number of degrees of freedom of the absolute nodal coordinate formulation model is reduced to half, the difference in the results obtained is less than 4%. It is important, however, to point out that unlike other large deformation finite element formulations, the absolute nodal coordinate formulation allows for using a relatively small number of elements in the case of very flexible structures.

Tables 2 and 3 show, respectively, the results corresponding to the first and second flap modes for different values of the angular velocity. Table 4 shows the results for the first

Journal ID: 11044, Article ID: 9070, Date: 2007-06-28, Proof No: 1

« MUBO 11044 layout: Small Condensed v.1.2 reference style: mathphys file: mubo9070.tex (Aiste) aid: 9070 doctopic: OriginalPaper class: spr-small-v1.1 v.2007/06/28 Prn:28/06/2007; 15:52 p. 18»

Table 4 Eigenfrequencies for the first lag mode at different angular velocities

Angular Veloc.	Geometrically exact beam model	ANCF_beam (continuum mechanic approach)	ANCF_beam (elastic line approach)	ANCF_beam (elastic line + Hellinger–Reissner approach)	ANCF_plate (continuum mechanic approach)
$0.0 * \omega_0$	26.34	30.54	25.34	25.22	26.72
$0.1 * \omega_0$	26.41	30.69	25.38	26.29	26.77
$0.2 * \omega_0$	26.49	30.76	25.45	26.37	26.90
$0.3 * \omega_0$	26.61	30.87	25.57	26.50	27.12
$0.4 * \omega_0$	26.79	31.03	25.74	26.68	27.43
$0.5 * \omega_0$	27.02	31.23	25.95	26.91	27.81
$0.6 * \omega_0$	27.29	31.48	26.20	27.20	28.27
$0.7 * \omega_0$	27.60	31.76	26.48	27.52	28.79
$0.8 * \omega_0$	27.94	32.07	26.80	27.88	29.38
$0.9 * \omega_0$	28.32	32.42	27.14	28.27	30.02
$1.0 * \omega_0$	28.72	32.80	27.52	28.66	30.70

lag mode. In the case of the first flap mode, the increase in the eigenfrequency due to the centrifugal effect is about 1000% when the angular velocity is equal to ω_0. For the second flap mode, this increase is about 300%. On the other hand, in the case of the first lag mode, the increase is only about 8%. These significantly different effects of the centrifugal forces on the flap and lag modes are mainly attributed to the direction of the centrifugal forces.

The use of a general continuum mechanics approach to formulate the elastic forces leads to a model that includes the ANCF coupled deformation modes, and consequently, leads to higher values of the eigenfrequencies as explained by Schwab and Meijaard [15]. However, when the effect of the centrifugal forces becomes more significant, the effect of the coupled deformation modes becomes less significant. The centrifugal forces tend to also increase the beam stiffness.

The use of an elastic line approach, in which the effect of the ANCF coupled deformation modes is eliminated, shows very good agreement with the solution obtained using the geometrically exact beam model. The very small differences in the results can be attributed to differences in the implementation, numerical procedures and convergence criteria. The numerical results obtained in this study also show a very good agreement between the results obtained using the two different nonlinear finite element formulations for higher order flap and lag modes. Recall that these two large deformation finite element formulations are conceptually different and lead to different beam and plate models, as previously discussed in this study.

As previously mentioned in this paper, the geometrically exact beam theory assumes that the beam cross section remains rigid, and as a consequence, the two normal strain components associated with the cross section deformation are equal to zero. Therefore, Poisson ratio does not enter into the formulation of the elastic forces when the geometrically exact beam theory is used. Table 5 shows the solution obtained using the absolute nodal coordinate formulation and the general continuum mechanics approach when the effect of the Poisson ratio is neglected and the angular velocity is equal to zero. It is clear from the results presented in this table that the eigenvalue solution obtained using the absolute nodal coordinate

Journal ID: 11044, Article ID: 9070, Date: 2007-06-28, Proof No: 1

Table 5 Effect of Poisson ratio

	Geometrically exact beam model	ANCF_beam (continuum mechanic approach) $\nu = 0.3$	ANCF_beam (continuum mechanic approach) $\nu = 0.0$
1st flap	2.64	3.07	**2.76**
2nd flap	16.55	19.46	**16.91**
1st lag	26.34	30.54	**26.45**

formulation and the general continuum mechanics approach is in a good agreement with the solution obtained using the geometrically exact beam model.

7 Summary and conclusions

In this study, the effect of the centrifugal forces on the eigenvalue solution obtained using two different nonlinear finite element formulations was examined. Both formulations can describe arbitrary rigid body motion and can be used for large deformation problems. The first formulation was based on a *geometrically exact beam theory*, which assumes that the cross section does not deform in its own plane and remains plane after deformation. The second formulation was based on the *absolute nodal coordinate formulation* (ANCF), which relaxes the assumption of the rigidity of the cross section. The results obtained in this study showed that when the ANCF coupled deformation modes are eliminated, one obtains a very good agreement between the solutions of the geometrically exact beam model and the absolute nodal coordinate formulation models when the effect of the centrifugal forces is considered. On the other hand, the use of a continuum mechanics approach to formulate the elastic forces leads to kinematic coupling between the deformation of the cross section and the bending deformation. While this coupling can be significant in the case of very flexible structures and/or plasticity problems, the coupled deformation modes tend to significantly increase the beam bending stiffness. The centrifugal forces also produce similar effect. As a consequence, as the effect of the centrifugal forces increases, the effect of the ANCF coupled deformation modes decreases and becomes less significant, as demonstrated by the results presented in this paper.

Acknowledgements This work was supported by the US Army Research Office, Research Triangle Park, North Carolina. This support is gratefully acknowledged.

Appendix 1

In this appendix, the shape functions used for the beam and plate elements based on the absolute nodal coordinate formulation are presented.

Beam element The shape function matrix $\mathbf{S}$ used to develop the beam element presented in this investigation is written as follows [20]:

$$\mathbf{S} = [\, S_1\mathbf{I} \quad S_2\mathbf{I} \quad S_3\mathbf{I} \quad S_4\mathbf{I} \quad S_5\mathbf{I} \quad S_6\mathbf{I} \quad S_7\mathbf{I} \quad S_8\mathbf{I} \,] \tag{64}$$

« MUBO 11044 layout: Small Condensed v.1.2 reference style: mathphys file: mubo9070.tex (Aiste) aid: 9070 doctopic: OriginalPaper class: spr-small-v1.1 v.2007/06/28 Prn:28/06/2007; 15:52 p. 20»

where $\mathbf{I}$ is the 3×3 identity matrix, and the shape functions S_i are defined as follows:

$$\left.\begin{aligned} &S_1 = 1 - 3\xi^2 + 2\xi^3, \qquad S_2 = l\left(\xi - 2\xi^2 + \xi^3\right), \qquad S_3 = l\eta(1-\xi), \\ &S_4 = l\zeta(1-\xi), \qquad S_5 = 3\xi^2 - 2\xi^3, \qquad S_6 = l\left(-\xi^2 + \xi^3\right), \\ &S_7 = l\eta\xi, \qquad S_8 = l\zeta\xi \end{aligned}\right\} \tag{65}$$

where $\xi = x/l$, $\eta = y/l$, $\zeta = z/l$, and l is the length of the element.

Plate element The shape function matrix $\mathbf{S}$ used to develop the plate element presented in this investigation is written as follows [11]:

$$\mathbf{S} = \begin{bmatrix} S_1\mathbf{I} & S_2\mathbf{I} & S_3\mathbf{I} & S_4\mathbf{I} & S_5\mathbf{I} & S_6\mathbf{I} & S_7\mathbf{I} & S_8\mathbf{I} \\ S_9\mathbf{I} & S_{10}\mathbf{I} & S_{11}\mathbf{I} & S_{12}\mathbf{I} & S_{13}\mathbf{I} & S_{14}\mathbf{I} & S_{15}\mathbf{I} & S_{16}\mathbf{I} \end{bmatrix} \tag{66}$$

where $\mathbf{I}$ is the 3×3 identity matrix, and the shape functions S_i are defined as follows:

$$\left.\begin{aligned} &S_1 = (2\xi+1)(\xi-1)^2(2\eta+1)(\eta-1)^2, && S_2 = l\xi(\xi-1)^2(2\eta+1)(\eta-1)^2, \\ &S_3 = w\eta(\xi-1)^2(2\xi+1)(\eta-1)^2, && S_4 = h\zeta(\xi-1)(\eta-1), \\ &S_5 = -\xi^2(2\xi-3)(2\eta+1)(\eta-1)^2, && S_6 = l\xi^2(\xi-1)(2\eta+1)(\eta-1)^2, \\ &S_7 = -w\eta\xi^2(2\xi-3)(\eta-1)^2, && S_8 = -h\xi\zeta(\eta-1), \\ &S_9 = \eta^2\xi^2(2\xi-3)(2\eta-3), && S_{10} = -l\eta^2\xi^2(\xi-1)(2\eta-3), \\ &S_{11} = -w\eta^2\xi^2(\eta-1)(2\xi-3), && S_{12} = h\zeta\xi\eta, \\ &S_{13} = -\eta^2(2\xi+1)(\xi-1)^2(2\eta-3), && S_{14} = -l\xi\eta^2(\xi-1)^2(2\eta-3), \\ &S_{15} = w\eta^2(\xi-1)^2(2\xi+1)(\eta-1), && S_{16} = -h\eta\zeta(\xi-1) \end{aligned}\right\} \tag{67}$$

where $\xi = x/l$, $\eta = y/w$, $\zeta = z/h$, l is the length, w is the width and h is the thickness of the element.

Appendix 2

In this appendix, the transformation matrix, which is used to define the nodal coordinates in the rotating frame, is obtained. The element nodal coordinate vector at node n is defined in the inertial frame as follows:

$$\mathbf{e}^n = \left[\mathbf{r}^{nT} \quad \left(\frac{\partial \mathbf{r}^n}{\partial x}\right)^T \quad \left(\frac{\partial \mathbf{r}^n}{\partial y}\right)^T \quad \left(\frac{\partial \mathbf{r}^n}{\partial z}\right)^T \right]^T. \tag{68}$$

This nodal coordinate vector consists of 4 three-dimensional absolute positions and gradient vectors which can be defined in the rotating frame by employing the following transformation:

$$\mathbf{a} = \mathbf{A}_0 \bar{\mathbf{a}} \tag{69}$$

where

$$\mathbf{A}_0 = \begin{bmatrix} \cos\theta & -\sin\theta & 0 \\ \sin\theta & \cos\theta & 0 \\ 0 & 0 & 1 \end{bmatrix} \tag{70}$$

Journal ID: 11044, Article ID: 9070, Date: 2007-06-28, Proof No: 1

« MUBO 11044 layout: Small Condensed v.1.2 reference style: mathphys file: mubo9070.tex (Aiste) aid: 9070 doctopic: OriginalPaper class: spr-small-v1.1 v.2007/06/28 Prn:28/06/2007; 15:52 p. 21»

and $\mathbf{a}$ and $\bar{\mathbf{a}}$ are vectors defined in the inertial and rotating frames, respectively; and θ is the angle that defines the orientation of the rotating frame with respect to the inertial frame. It follows that, when the absolute nodal coordinate formulation is used, the relationship between the absolute coordinates defined in the inertial frame and the absolute coordinates defined in the rotating frame can be, in general, written as

$$\mathbf{e} = \mathbf{A}\mathbf{q} \tag{71}$$

where

$$\mathbf{A} = \begin{bmatrix} \mathbf{A}_0 & \mathbf{0} & \dots & \mathbf{0} \\ \mathbf{0} & \mathbf{A}_0 & \dots & \mathbf{0} \\ \vdots & \vdots & \ddots & \vdots \\ \mathbf{0} & \mathbf{0} & \dots & \mathbf{A}_0 \end{bmatrix}. \tag{72}$$

In this equation, $\mathbf{A}$ has dimension equal to the total number of nodal coordinates of the beam. Note that for one element e with volume V^e and mass density ρ^e, one has

$$\mathbf{A}^T\mathbf{M}\mathbf{A} = \begin{bmatrix} \mathbf{A}_0^T & \mathbf{0} & \dots & \mathbf{0} \\ \mathbf{0} & \mathbf{A}_0^T & \dots & \mathbf{0} \\ \vdots & \vdots & \ddots & \vdots \\ \mathbf{0} & \mathbf{0} & \dots & \mathbf{A}_0^T \end{bmatrix} \times \int_{V^e} \rho^e \begin{bmatrix} S_1^2\mathbf{I} & S_1S_2\mathbf{I} & \dots & S_1S_n\mathbf{I} \\ S_2S_1\mathbf{I} & S_2^2\mathbf{I} & \dots & S_2S_n\mathbf{I} \\ \vdots & \vdots & \ddots & \vdots \\ S_nS_1\mathbf{I} & S_nS_2\mathbf{I} & \dots & S_n^2\mathbf{I} \end{bmatrix} dV^e \begin{bmatrix} \mathbf{A}_0 & \mathbf{0} & \dots & \mathbf{0} \\ \mathbf{0} & \mathbf{A}_0 & \dots & \mathbf{0} \\ \vdots & \vdots & \ddots & \vdots \\ \mathbf{0} & \mathbf{0} & \dots & \mathbf{A}_0 \end{bmatrix} \tag{73}$$

which can be written as

$$\mathbf{A}^T\mathbf{M}\mathbf{A} = \int_{V^e} \rho^e \begin{bmatrix} \mathbf{A}_0^TS_1^2\mathbf{A}_0 & \mathbf{A}_0^TS_1S_2\mathbf{A}_0 & \dots & \mathbf{A}_0^TS_1S_n\mathbf{A}_0 \\ \mathbf{A}_0^TS_2S_1\mathbf{A}_0 & \mathbf{A}_0^TS_2^2\mathbf{A}_0 & \dots & \mathbf{A}_0^TS_2S_n\mathbf{A}_0 \\ \vdots & \vdots & \ddots & \vdots \\ \mathbf{A}_0^TS_nS_1\mathbf{A}_0 & \mathbf{A}_0^TS_nS_2\mathbf{A}_0 & \dots & \mathbf{A}_0^TS_n^2\mathbf{A}_0 \end{bmatrix} dV^e. \tag{74}$$

Using the fact that $\mathbf{A}_0$ is an orthogonal matrix, the preceding equation shows that

$$\mathbf{A}^T\mathbf{M}\mathbf{A} = \mathbf{M}. \tag{75}$$

Similarly, one can write

$$\mathbf{A}^T\mathbf{M}\dot{\mathbf{A}} = \int_{V^e} \rho^e \begin{bmatrix} \mathbf{A}_0^TS_1^2\dot{\mathbf{A}}_0 & \mathbf{A}_0^TS_1S_2\dot{\mathbf{A}}_0 & \dots & \mathbf{A}_0^TS_1S_n\dot{\mathbf{A}}_0 \\ \mathbf{A}_0^TS_2S_1\dot{\mathbf{A}}_0 & \mathbf{A}_0^TS_2^2\dot{\mathbf{A}}_0 & \dots & \mathbf{A}_0^TS_2S_n\dot{\mathbf{A}}_0 \\ \vdots & \vdots & \ddots & \vdots \\ \mathbf{A}_0^TS_nS_1\dot{\mathbf{A}}_0 & \mathbf{A}_0^TS_nS_2\dot{\mathbf{A}}_0 & \dots & \mathbf{A}_0^TS_n^2\dot{\mathbf{A}}_0 \end{bmatrix} dV^e. \tag{76}$$

Using the identities of (57), and the fact that $\dot{\mathbf{A}}_0 = \dot{\theta}\mathbf{A}_{0\theta}$; the preceding equation shows that $\mathbf{A}^T\mathbf{M}\dot{\mathbf{A}}$ is a constant matrix if the angular velocity $\dot{\theta}$ is constant, which is the case in the analysis presented in this paper.

Journal ID: 11044, Article ID: 9070, Date: 2007-06-28, Proof No: 1

« MUBO 11044 layout: Small Condensed v.1.2 reference style: mathphys file: mubo9070.tex (Aiste) aid: 9070 doctopic: OriginalPaper class: spr-small-v1.1 v.2007/06/28 Prn:28/06/2007; 15:52 p. 22»

Following a similar procedure, one can also write

$$\mathbf{A}^T\mathbf{M}\ddot{\mathbf{A}} = \int_{V^e} \rho^e \begin{bmatrix} \mathbf{A}_0^T S_1^2 \ddot{\mathbf{A}}_0 & \mathbf{A}_0^T S_1 S_2 \ddot{\mathbf{A}}_0 & \dots & \mathbf{A}_0^T S_1 S_n \ddot{\mathbf{A}}_0 \\ \mathbf{A}_0^T S_2 S_1 \ddot{\mathbf{A}}_0 & \mathbf{A}_0^T S_2^2 \ddot{\mathbf{A}}_0 & \dots & \mathbf{A}_0^T S_2 S_n \ddot{\mathbf{A}}_0 \\ \vdots & \vdots & \ddots & \vdots \\ 1\mathbf{A}_0^T S_n S_1 \ddot{\mathbf{A}}_0 & \mathbf{A}_0^T S_n S_2 \ddot{\mathbf{A}}_0 & \dots & \mathbf{A}_0^T S_n^2 \ddot{\mathbf{A}}_0 \end{bmatrix} dV^e. \tag{77}$$

Using the identities of (57), it can be shown that the matrix $\mathbf{A}^T\mathbf{M}\ddot{\mathbf{A}}$ is constant under the assumptions stated in this paper.

References

1. Bauchau, O.A.: Computational schemes for flexible nonlinear multibody systems. Multibody Syst. Dyn. **2**, 169–225 (1998)
2. Bauchau, O.A., Bottasso, C.L., Nikishkov, Y.G.: Modeling rotorcraft dynamics with finite element multibody procedures. J. Math. Comput. Modeling **33**, 1113–1137 (2001)
3. Berzeri, M., Shabana, A.A.: Study of the centrifugal stiffening effect using the finite element absolute nodal coordinate formulation. Multibody Syst. Dyn. **7**, 357–387 (2002)
4. Cesnik, C.E.S., Hodges, D.H., Sutyrin, V.G.: Cross-sectional analysis of composite beams including large initial twist and curvature effects. AIAA J. **34**, 1913–1920 (1996)
5. Crisfield, M.A.: Non-Linear Finite Element Analysis of Solids and Structures, vol. I: Essentials. Wiley, New York (1997)
6. Garcia-Vallejo, D., Sugiyama, H., Shabana, A.A.: Finite element analysis of the geometric stiffening effect, part 1: a correction in the floating frame of reference formulation. IMechE J. Multibody Dyn. **219**, 187–202 (2004)
7. Garcia-Vallejo, D., Sugiyama, H., Shabana, A.A.: Finite element analysis of the geometric stiffening effect, part 2: non-linear elasticity. IMechE J. Multibody Dyn. **219**, 203–211 (2004)
8. Hodges, D.H.: A review of composite rotor blade modeling. AIAA J. **28**, 561–565 (1990)
9. Hussein, B., Sugiyama, H., Shabana, A.A.: Coupled deformation modes in the large deformation finite element analysis: problem definition. ASME J. Comput. Nonlinear Dyn. **2**, 146–154 (2007)
10. Johnson, W.: Helicopter Theory. Princeton University Press, New Jersey (1980)
11. Mikkola, A.M., Shabana, A.A.: A non-incremental procedure for the analysis of large deformation of plates and shells in mechanical systems application. Multibody Syst. Dyn. **9**, 283–309 (2003)
12. Pascal, M.: Some open problems in dynamic analysis of flexible multibody systems. Multibody Syst. Dyn. **5**, 315–334 (2001)
13. Reissner, E.: On a variational theorem for finite elastic deformation. J. Math. Phys. **32**, 129–135 (1953)
14. Schilhans, M.J.: Bending frequency of a rotating cantilever beam. Trans. ASME J. Appl. Mech. **25**, 28–30 (1958)
15. Schwab, A.L., Meijard, J.P.: Comparison of three-dimensional flexible beam elements for dynamic analysis: finite element method and absolute nodal coordinate formulation. In: Proceedings of ASME International Design Engineering Technical Conferences and Computer Information in Engineering Conference (DETC2005/ MSNDC-85104), Long Beach, CA, USA (2005)
16. Shabana, A.A.: Dynamics of Multibody Systems, 3rd edn. Cambridge University Press, Cambridge (2005)
17. Shabana, A.A., Yakoub, R.Y.: Three dimensional absolute nodal coordinate formulation for beam elements: Theory. ASME J. Mech. Des. **123**, 606–613 (2001)
18. Wallrapp, O., Schwertassek, R.: Representation of geometric stiffening in multibody system simulation. Int. J. Numer. Methods Eng. **32**, 1833–1850 (1991)
19. Wu, S.C., Haug, E.J.: Geometric non-linear substructuring for dynamics of flexible mechanical systems. J. Numerical Methods Eng. **26**, 2211–2226 (1988)
20. Yakoub, R.Y., Shabana, A.A.: Three-dimensional absolute nodal coordinate formulation for beam elements: implementation and applications. ASME J. Mech. Des. **123**, 614–621 (2001)

Journal ID: 11044, Article ID: 9070, Date: 2007-06-28, Proof No: 1